

Effect of Mn^{2+} on the electrical nonlinearity of (Ni, Nb)-doped SnO_2 varistors

Changpeng Li*, Jinfeng Wang, Wenbin Su, Hongcun Chen, Weilie Zhong, Peilin Zhang

Department of Physics, Shandong University, Jinan 250100, PR China

Received 25 September 2000; received in revised form 2 February 2001; accepted 12 February 2001

Abstract

The reason that the (Ni, Nb)-doped SnO_2 varistors exhibit poorer densification and electrical nonlinearity than the (Co, Nb)-doped SnO_2 varistors is explained. The effect of Mn^{2+} on the electrical nonlinear properties of SnO_2 based ceramics were investigated. The sample doped with 0.10 mol% MnCO_3 exhibits the highest reference electrical field of 686.89 V/mm, the highest electrical nonlinear coefficient of 12.9, which is consistent with the highest grain-boundary defect barriers. It can be explained by the effect of the substitution of Sn^{4+} for Mn^{2+} , which facilitate the formation of the defect barriers, and the maximum of the substitution. The shrinkage rates increase with the doping of MnCO_3 , although the sample doped with 0.5 mol% MnCO_3 appears the highest density ($\rho = 6.87 \text{ g/cm}^3$). In order to illustrate the grain boundary barriers formation in $\text{SnO}_2\text{.Ni}_2\text{O}_3\text{.Nb}_2\text{O}_5\text{.MnCO}_3$ varistors, a grain-boundary defect barrier model was introduced. © 2001 Elsevier Science Ltd and Techna S.r.l. All rights reserved.

Keywords: C. Electrical properties; E. Varistors; Tin oxide; Manganese oxide

1. Introduction

Varistors are electric devices whose primary functions are to sense and limit transient voltage surges and to do so repeatedly without being destroyed. The most important property of a varistor is its nonlinear current–voltage characteristic, which can be expressed by the equation $I = KV^\alpha$, where α is the nonlinear coefficient, a vital parameter used to scale the nonlinearity. The greater the value of α , the better the device.

Varistors based on ZnO, which exhibit good nonlinearity electrical properties, have been most extensively studied [1,2]. At the same time, varistors based on other ceramic systems are also under investigation, because of the need for even better properties. Tin dioxide (SnO_2) is an *n*-type semiconductor with the rutile structure [3]. It is characterized by low densification during sintering, an advantage for gas sensor devices [4,5]. Dense SnO_2 -based ceramics can be achieved by introducing dopants [6] or by hot isostatic pressure processing [7]. S.A.Pianaro reported that dopants with valence +2 could substitute for tin ions and create defects in the crystalline

lattice, which will promote densification of SnO_2 ceramics [8]. The processing of SnO_2 based material with high-density enables its use in other types of electronic devices such as varistors, as reported by Pianaro et al. [8].

In the previous work, we found that (Ni, Nb)-doped SnO_2 ceramics exhibits the electrical nonlinearity. However, these ceramics appears lower density (84.9% of the theoretical density of SnO_2) and poorer electrical nonlinear properties ($\alpha = 6.0$), which cannot meet the requirement of the market. In this paper, the effect of Mn^{2+} on the electrical nonlinearity was investigated mainly by measuring the densities, the properties of the grain boundary barrier and the nonlinear current-vs-voltage (*I–V*) characteristics.

2. Experimental procedure

The raw chemicals in the present study were analytical grades of SnO_2 (99.5%), Ni_2O_3 (99%), Nb_2O_5 (99.95%) and MnCO_3 (99%). The compositions investigated in the present work were $(100-0.05-0.75-X) \% \text{SnO}_2$ 4 0.75% Ni_2O_3 + 0.05% Nb_2O_5 + *X*% MnCO_3 , where *X* = 0, 0.05, 0.10, 0.25, 0.50, 1.0. The chemicals were weighed and wet-milled in a polyethylene bottle with ZrO_2 balls

* Corresponding author.

E-mail address: physlicp@263.net (C. Li).

for 14 h in deionized water and some alcohol. The milled powder slurry was stirred and simultaneously dried under an infrared lamp to remove water and then forced to pass a 100-mesh sieve. The granulated powder was pressed into disks 15 mm in diameter and 1.5 mm in thickness at a pressure of 160 MPa, which were sintered at temperature 1450°C for 1 h, and cooled at a constant rate of 5°C/mm above 1100°C during sintering. The green compacts were put into an Al₂O₃ crucible and fully surrounded with powder of matching composition.

Apparent densities were determined after sintering by Archimedes methods. X-ray powder diffraction analyses were performed to investigate the phase compositions in the SnO₂.Ni₂O₃.Nb₂O₅.MnCO₃ varistors. For microstructural characterization, the samples were polished, thermally etched and analyzed in a scanning electron microscope (SEM). The mean grain sizes were determined by the intercept method. For electrical properties measurement, silver electrodes were made on both surfaces of the sintered pellets. And for electrical characterization of current density versus applied electrical field, a semiconductor I - V graph (QT2) was used.

3. Results

X-ray powder diffraction analyses demonstrated that there were no second phases in the SnO₂.Ni₂O₃.Nb₂O₅.MnCO₃ varistors, which is in agreement with Pianaro et al. [8] who reported a single-phase system for the SnO₂.CoO.Nb₂O₅ system. The single-phase property makes the SnO₂ system less affected by the sintering crafts than the system of ZnO or TiO₂ ceramics. A SEM is also used to investigate the micromechanism of the samples, which shows that the sample doped with 0.10 mol% MnCO₃ exhibits the smallest grain sizes.

The nonlinear characteristics in electrical properties of the SnO₂.Ni₂O₃.Nb₂O₅.MnCO₃ ceramics are shown

in Fig. 1. The nonlinear coefficient α was obtained by [9]

$$\alpha = \frac{\log(I_2/I_1)}{\log(V_2/V_1)} \quad (1)$$

where V_1 and V_2 are, respectively, the voltage at current I_1 and I_2 . It is shown from Table 1 that the SnO₂ varistor doped with Ni₂O₃ exhibits lower density and poorer electrical nonlinearity than the SnO₂ varistor doped with CoO. Fig. 1 shows I - V characteristics of the samples doped with different amounts of MnCO₃. It is shown that the sample doped with 0.10 mol% MnCO₃ exhibits the highest reference electrical field ($E_B = 686.89$ V/mm) and the highest electrical nonlinearity ($\alpha = 12.9$). The reference voltage is proportional to the thickness of the pellet, which suggests that the non-ohmic behavior is a bulk property of SnO₂ ceramics, and not a property of the ceramic-electrode interface [10].

Considering the Schottky type conduction model [11], plots of $\ln J$ against $E^{1/2}$ of the SnO₂ based varistor with different MnCO₃ dopants, as Fig. 2, can be built up to determine values for ϕ_B and β . The barrier height (ϕ_B)

Table 1

The contrast of properties between the (Ni, Nb)-doped SnO₂ varistor and the (Co, Nb)-doped SnO₂ varistor

	α	d_r (g/cm ³) ^a	Relative density (%)	E_B (V/mm)	ϕ_B (eV)	$\beta \times 10^3$ (V ^{-1/2} cm ^{1/2})	Sintering temperature (°C)
1.0 mol% CoO	8	5.90	84.9	1870	0.49	7.10	1350
0.75 mol% Ni ₂ O ₃	5.9	6.77	97.4	120	0.44	6.40	1500

^a Theoretical density of SnO₂, $d_t = 6.95$ g/cm³.

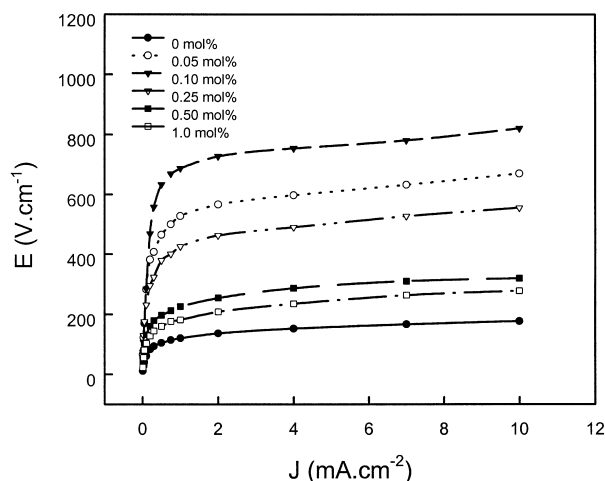


Fig. 1. I - V characteristics of samples with different MnCO₃ dopants.

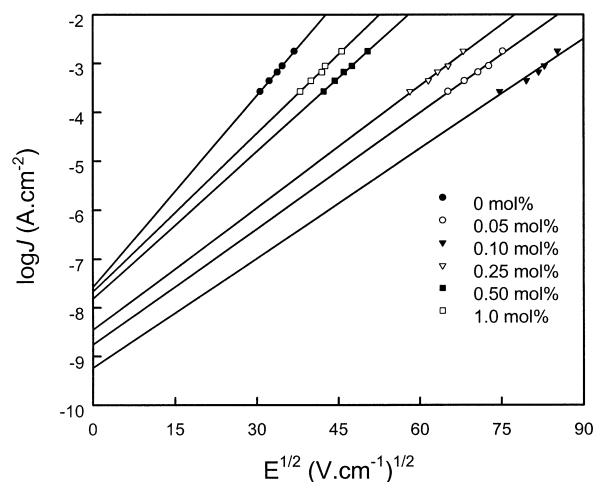


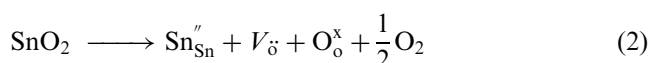
Fig. 2. Characteristic plots of $\ln J \times E^{1/2}$ for sample with different MnCO₃ dopants.

can be obtained from the intersection of the extrapolated lines of the plot with the voltage axis, and the relative magnitude of constant β , which is inverse to ω , can be derived from the slopes of the plots. Values of ϕ_B and ω are shown in Table 2. It is found that the sample doped with 0.10 mol% MnCO_3 exhibits the highest grain defect barriers, which is consistent with the best electrical nonlinearity of that composition.

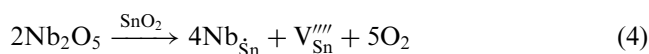
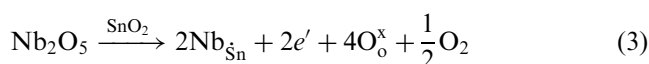
Table 2 also shows the variation of densities and the shrinkage rates with different dopants of MnCO_3 . It is shown that the shrinkage rates increase with the doping of MnCO_3 , although the sample doped with 0.5 mol% MnCO_3 appears the highest density ($\rho = 6.87 \text{ g/cm}^3$).

4. Discussion

For the doped SnO_2 varistors, defect formation by donors and acceptors in the SnO_2 matrix should be responsible for the origin of the potential barriers at grain boundaries, because there are no secondary phases precipitated at the grain boundaries. Thus, in similar with the SnO_2 based varistor doped with (Nb, Co), the following equilibrium reaction may be written [12,13]:

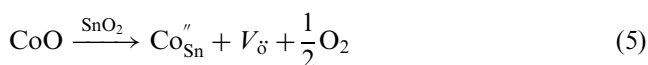


The addition of Nb_2O_5 in small amounts to the SnO_2 ceramics leads to the concentration of e' and V_{Sn}'''' , which increase the electronic conductivity in the SnO_2 lattice according to:

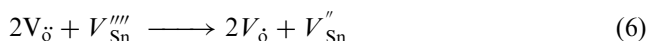


For diffusion-controlled processes like sintering, the slowest diffusion species (V_{O}^{\times}) should determine the overall rate of the sintering [14]. The introduction of Ni_2O_3 or CoO leads to the densification and good

electrical nonlinearities according to:

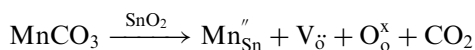


The oxygen vacancies can combine with tin vacancies according to the reaction:



In contrast to the radius of Co^{2+} ($r = 0.074 \text{ nm}$), the radius of Ni^{3+} ($r = 0.062 \text{ nm}$) is much smaller than the radius of Sn^{4+} ($r = 0.07 \text{ nm}$). Co^{2+} exhibits a greater affinity with the oxygen ions (O^{2+}) than Ni^{3+} . Thus, Co^{2+} enters into the lattice and the grain interface more easily, together with the greater amount of oxygen vacancies introduced by every mol acceptor ion, which facilitate the concentration of oxygen vacancies and the formation of solid solution, leading to the increase of the sintering rate and the densities. The concentration of defects, increased by the substitution of Sn^{4+} with Co^{3+} , also facilitate the formation of the grain-boundary defect barriers, which is responsible for the electrical nonlinearity of the samples. Thus, the (Ni, Nb)-doped SnO_2 varistors exhibit poorer densification and electrical nonlinearities.

The dopants of Mn^{2+} are acceptors for SnO_2 and are usually ionically compensated by the formation of oxygen vacancies. Thus, the following reaction is proposed similar to Co^{2+} :



Every mol dopants of Mn^{2+} , with an ion radius of 0.080 nm , can create one mol oxygen vacancies, consistent with Co^{2+} . MnCO_3 also has a low melting point, which makes Mn^{2+} form a solid solution with Sn^{4+} more easily. Thus, the introduction of Mn^{2+} increases the sintering rate, which increase the densities of the samples and decrease the best sintering temperature accordingly. However, the sample doped with 0.5 mol%

Table 2
Some characteristics of the samples with different amounts of MnCO_3 dopants

MnCO_3 (mol%)	α	d_t (g/cm^3) ^a	Relative density (%)	E_B (V/mm)	ϕ_B (eV)	$\beta \times 10^3$ ($\text{V}^{-1/2} \text{ cm}^{1/2}$)	Shrinkage rate
0	5.97	5.16	74.2	120.35	0.44	6.40	0.043
0.05	9.70	5.50	79.1	528.3	0.51	4.28	0.070
0.10	12.94	5.87	84.5	686.89	0.56	4.10	0.084
0.25	8.67	6.33	91.1	425.53	0.50	4.35	0.108
0.50	6.61	6.87	98.8	225.99	0.48	5.16	0.135
1.0	5.38	6.80	97.8	181.44	0.46	5.66	0.139

^a Theoretical density of SnO_2 , $d_t = 6.95 \text{ g/cm}^3$.

MnCO_3 appears the highest density, although the shrinkage rates increase with the doping of MnCO_3 . It can be explained that the dopants of MnCO_3 will be evaporated at a high temperature because of its low melting point. The more of the amount of MnCO_3 , the more of the amount of evaporation. The densities are determined by the common effects of the sintering rate and the evaporation.

The introduction of Mn^{2+} also increases the concentration of defect ions, which facilitate the formation of the grain-boundary defect barriers. Thus, the height and the width of the defect barrier increase with the introduction of Mn^{2+} , which leads to higher electrical non-linear coefficients. The sample doped with 0.10 mol% MnCO_3 appears the highest nonlinear coefficient, which is consistent with the highest defect barriers.

The SEM shows that the grain sizes of the samples decrease with the introduction of MnCO_3 until the amount of the dopant reaches 0.10 mol%. It can be explained that the introduction of Mn^{2+} increases the height and the width of the boundary barriers, which blocks the growth of the grains. According to the boundary barrier model, the reference voltage barrier, V_B , for a varistor is determined by the mean number of barriers \bar{n} in series multiplied by v_b , that is [13].

$$V_B = \bar{n} \cdot v_b, \quad (7)$$

where v_b is the voltage barrier at the grain boundary; \bar{n} is in inverse proportion to the grain sizes. The sample doped with 0.10 mol% MnCO_3 , with higher defect barriers and smaller grain sizes, appears higher reference electrical field.

However, the substitution of Sn^{4+} with Mn^{2+} exists as a maximum. When the introduction of Mn^{2+} exceeds this limit, the superfluous Mn^{2+} , which cannot substitute Sn^{4+} further, will segregate to grain boundary interfaces. Thus, the segregation of Mn^{2+} blocks the building and transportation of e^- and other defects, which will have an effect on the properties of the SnO_2 based samples, contrary to the substitution of Sn^{4+} with Mn^{2+} , as shown in the figures and Table 2. Thus, the height and the width of the grain-boundary defect barrier decrease with the introduction of Mn^{2+} , which leads to the poorer electrical nonlinearities. The grain sizes increase because the height and the width of the defect barriers decrease with the dopants of Mn^{2+} , which, together with the decrease of the defect barriers, leads to the decrease of the reference electrical field.

Gupla and Carlson developed a grain boundary defect model for ZnO varistors analogous to the band model comprising the Schottky barriers [15]. In order to illustrate the grain-boundary barriers formation in $\text{SnO}_2 \cdot \text{Ni}_2\text{O}_3 \cdot \text{Nb}_2\text{O}_5 \cdot \text{MnCO}_3$ varistors, an analogy to this model can be considered, as in Fig. 3. In this model

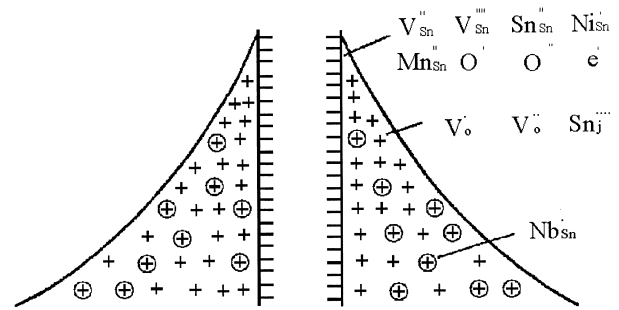


Fig. 3. The grain-boundary defect barrier model for $\text{SnO}_2 \cdot \text{Ni}_2\text{O}_3 \cdot \text{Nb}_2\text{O}_5 \cdot \text{MnCO}_3$ varistors.

there is a large negative charge concentration at the SnO_2 grain surface that should be attributed to tin vacancies (V_{Sn}'''' , V_{Sn}''), electrons (e^-) and the substitution of tin ions by nickel and manganese at the interface (Ni_{Sn}' , Mn_{Sn}''). These electrical charges are balanced by positive charges distributed in the depletion layer region, near the interface, with width ω . These positive charges could be oxygen vacancies (V_{O}' , V_{O}) and/or interstitial tin ions (Sn_j'') as well as the positive defects promoted by the solid solution formation of niobium in SnO_2 (Nb_{Sn}). During the sintering and cooling processes the diffusion of molecular oxygen through the grain boundary may occur and then it reacts with the negative defects, then the resultants of O' and O'' also play an important effect on the formation of depletion layer region. The depletion layers at grain boundaries, together with negative charge concentration at the SnO_2 grain surface, form a voltage barrier for the electronic transport. This transport occurs by tunneling and is responsible for the nonlinear ohmic characteristics [16].

5. Conclusions

The main conclusions are as follows:

1. The reason that the (Ni, Nb)-doped SnO_2 varistors exhibits a poorer densification and electrical non-linearity than the (Co, Nb)-doped SnO_2 varistors is explained.
2. The effect of Mn^{2+} on the electrical nonlinear properties of SnO_2 based ceramics were investigated. The sample doped with 0.10 mol% MnCO_3 exhibits the highest reference electrical field of 686.89 V/mm, the highest electrical nonlinear coefficient of 12.9, which is consistent with the highest grain-boundary defect barriers.
3. In order to illustrate the grain boundary barriers formation in $\text{SnO}_2 \cdot \text{Ni}_2\text{O}_3 \cdot \text{Nb}_2\text{O}_5 \cdot \text{MnCO}_3$ varistors, a grain-boundary defect barrier model was introduced.

References

- [1] T.K. Gupta, Application of zinc oxide varistors, *J. Am. Ceram. Soc.* 73 (7) (1990) 1817.
- [2] P.R. Emtage., The physics of zinc oxide varistors, *J. Appl. Phys.* 48 (10) (1977) 4372.
- [3] J.G. Fagan, V.R.W. Amar Akoon, Reliability and reproducibility of ceramic sensors: part III, humidity sensors, *Am. Ceram. Soc. Bull.* 72 (3) (1993) 119.
- [4] Joss. H.D. Initial Stage Sintering of Tin Oxide, MSc thesis, University of Washington, Seattle, WA, 1975.
- [5] J.A. Varela, O.J. Whitemore., E. Longo, Pore size evolution during sintering of ceramic oxide, *Ceram. Int.* 16 (3) (1990) 177.
- [6] S. Zuca, M. Terzi, M. Zaharescu, Contribution to the study of SnO₂-based ceramics: part II, effect of various oxide additives on the sintering capacity and electrical conductivity of SnO₂, *J. Mater. Sci.* 26 (1991) 1673.
- [7] S.J. Park., K. Hirota, H. Yamamura, Densification of non-additive SnO₂ by hot isostatic pressing, *Ceram. Int.* 10 (3) (1984) 115.
- [8] S.A. Pianaro, P.R. Bueno, E. Longo, A new SnO₂-based varistor system, *J. Mater. Sci. Lett.* 14 (1995) 692.
- [9] J.F. Wang, Nonlinear electrical behaviour of the TiO₂-Sb₂O₃ system, *Chin. Phys. Lett.* 17 (7) (2000) 530.
- [10] V. Makarov, M. Trontelj., Novel varistor material based on tungsten oxide, *J. Mater. Sci. Lett.* 13 (1994) 937.
- [11] S.A. Pianaro, Effect of Bi₂O₃ addition on the microstructure and electrical properties of the SnO–CoO–Nb₂O₅ varistor system, *J. Mater. Sci. Lett.* 16 (1997) 634.
- [12] E.R. Leite, A.M. Nascimento, The influence of sintering process and atmosphere on the non-ohmic properties of SnO₂ based varistor, *J. Mater. Sci.* 10 (1999) 321.
- [13] J.F. Wang, Nonlinear electrical behaviour of the SnO₂-Ni₂O₃-Ta₂O₅ system, *J. Mater. Sci. Lett.* 18 (1999).
- [14] J.A. Cerri, E.R. Leite, D. Gouvea., E. Longo, Effect of cobalt(II) oxide and manganese(IV) oxide on sintering of tin(IV) oxide, *J. Am. Ceram. Soc.* 79 (3) (1996) 799.
- [15] T.K. Gupta, W.G. Carlson, A grain-boundary defect model for instability/stability of a ZnO varistor, *J. Mater. Sci.* 20 (1983) 3487.
- [16] Y.J. Wang, Electrical properties of SnO₂-ZnO–Nb₂O₅ varistor system, *J. Phys. D: Appl. Phys.* 33 (2000) 96.